Strength and Elasticity of SiO_2 across the Stishovite–$CaCl_2$-type Structural Phase Boundary

Sean R. Shieh* and Thomas S. Duffy
Department of Geosciences, Princeton University, Princeton, New Jersey 08544

Baosheng Li
Mineral Physics Institute, SUNY at Stony Brook, Stony Brook, New York 11794

(Received 10 July 2002; published 3 December 2002)

Radial x-ray diffraction experiments were conducted under nonhydrostatic compression on SiO_2 to 60 GPa in a diamond anvil cell. This ratio of differential stress to shear modulus t/G is 0.019(3)–0.037(5) at $P = 15$–60 GPa. The ratio for octahedrally coordinated stishovite is lower by a factor of about 2 than observed in four-coordinated silicates. Using a theoretical model for the shear modulus, the differential stress of stishovite is found to be 4.5(1.5) GPa below 40 GPa and to decrease sharply as the stishovite–$CaCl_2$-type phase transition boundary is approached. Inversion of measured lattice strains provides direct experimental evidence for softening of C_{11}-C_{12}.

DOI: 10.1103/PhysRevLett.89.255507 PACS numbers: 62.50.+p, 61.10.–i, 62.20.Fe, 91.60.–x

The properties of stishovite, the octahedrally coordinated polymorph of silica in the rutile structure, are of broad interest [1]. Stishovite has been observed naturally in meteorites [2], and its presence in the deep Earth is inferred from associations in diamond inclusions [3]. It may contribute to unexplained seismic structure in the Earth's mantle [4]. More generally, it is regarded as a prototype for the six-coordinated silicates that are of fundamental importance in solid-state physics, chemistry, and geophysics [5]. The extensive polymorphism in dense silica is an area of particular focus [1,6,7]. Stishovite is known to transform to an orthorhombic $CaCl_2$-type structure at 50 ± 3 GPa on the basis of theoretical calculations [8–11], Raman spectroscopy [12], and x-ray diffraction studies [13,14]. The study of elastic instabilities is important for understanding phase transformations, and the stishovite–$CaCl_2$-type transition, which is driven by an instability of an elastic shear modulus, has attracted much attention in this regard [8,12].

Polycrystalline stishovite is also among the strongest known oxides [15], and understanding its elastic and rheological properties is fundamental to the search for new superhard materials [16,17]. As the strength, equation of state, and refractory properties are expected to vary with coordination number in the silica system (e.g., [18]), investigation of the high-pressure polymorphs is especially important. At present, direct experimental measurements of the elastic properties, strength, and plastic deformation behavior of stishovite at high pressures are limited [19,20]. In this study, we use lattice strain measurements under nonhydrostatic compression in a diamond anvil cell [21–24] to examine dense SiO_2 over a broad pressure range.

The sample was synthesized in the 2000-ton uniaxial split-sphere apparatus at the SUNY Stony Brook High-Pressure Laboratory. X-ray diffraction revealed the material to be pure stishovite with no detectable impurities. The sample was ground into fine powder (~ 1 μm) and loaded into a 90-μm diam hole of a Be gasket that was preindented to 20–30 μm thickness. A 10–15 μm foil of Au was placed on top within ~ 5 μm of the sample center. This foil served as both a pressure marker [23] and as a reference for the x-ray position. A diamond anvil cell was used to compress the sample under intentionally nonhydrostatic conditions (i.e., no pressure transmitting medium). Radial x-ray diffraction experiments [21–24] were performed at the X17C beam line of the National Synchrotron Light Source. The incident x-ray beam was focused by a pair of Kirkpatrick-Baez mirrors to approximately 10×15 μm and directed through the Be gasket and the sample. At each loading step, a series of diffraction patterns was obtained by rotating the diamond cell about an axis that bisects 2θ, the angle between the incident x-ray beam and the detector. This allows for measurement of lattice strain at any angle with respect to the loading axis. Experiments were performed using energy dispersive x-ray diffraction and a solid-state Ge detector fixed at $2\theta = 12°$. The collecting time was 5–30 min for each spectrum. Spectra were collected only after sufficient time elapsed after pressurization (typically 1–2 h) such that stress relaxation was observed to be negligible.

The data were analyzed using lattice strain theory [21–24], which relates the anisotropy of the measured lattice strains to the supported differential stress and the elastic stiffness coefficients. The stress tensor in a diamond cell under nonhydrostatic loading can be characterized by the stress along the diamond cell axis, σ_3, and the radial stress, σ_1. The differential stress, t, is given by $\sigma_3 - \sigma_1$. The supported differential stress is a lower bound to the yield strength. The measured d spacing is given by [21,22]

$$d_m(hkl) = d_p(hkl)[1 + (1 - 3\cos^2\psi)Q(hkl)], \quad (1)$$

where $d_m(hkl)$ is the measured interplanar spacing for plane (hkl), $d_p(hkl)$ is the d spacing resulting from the hydrostatic component of stress, ψ is the angle between the diffracting plane normal and the loading direction, and

$$Q(hkl) = (t/3)\{\alpha[2G_R^X(hkl)]^{-1} + (1-\alpha)(2G_V)^{-1}\}. \quad (2)$$

$G_R^X(hkl)$ is the x-ray shear modulus under the Reuss (isostress) condition and G_V is the shear modulus under Voigt (isostrain) conditions. The parameter α, which can vary between 0 and 1, is the weighting factor for the relative degree of stress and strain continuity across grain boundaries. We assumed that the sample here was under isostress (Reuss) conditions. We note that the measured d spacing is equivalent to the d spacing under hydrostatic stress when $1 - 3\cos^2\psi = 0$ or $\psi = 54.7°$. The differential stress can be estimated from the shear modulus and the average $Q(hkl)$ value from all measured reflections by [21,22]

$$t = 6G\langle Q(hkl)\rangle. \quad (3)$$

The diffraction patterns (Fig. 1) obtained at $\psi = 0°$ and 90° describe the maximum and minimum strain in the sample. The peaks shift to lower energies as the angle from the loading axis increases. As expected, the d spacings increase linearly with $1 - 3\cos^2\psi$.

By assuming that the measured d spacings correspond to volume compression under hydrostatic stress, data at $\psi = 0°$, 54.7°, and 90° can be compared with previous equation of state data under quasihydrostatic [1,13,25,26] and nonhydrostatic [6] conditions (Fig. 2). The equation of state at 54.7° generally agrees with previous quasihydrostatic measurements [1,13,25,26], but appears slightly less compressible than the measurements of Hemley *et al.* [1] above 30 GPa. Fitting the 54.7° data below 50 GPa to a Birch-Manurghan equation of state yields a pressure derivative of the bulk modulus, K_0', of 4.6(1) when the bulk modulus, K_0, is fixed at 304 GPa [25]. This pressure derivative is intermediate to previous values from compression using a He medium ($K_0' = 3.98$) [1], ultrasonic elasticity ($K_0' = 5.1$) [25], and direct shock compression of stishovite ($K_0' = 5.0$) [27], and in good agreement with very recent measurements from quenched laser heated samples [$K_0' = 4.8(2)$] [26]. As expected, the equation of state at 90° agrees with previous nonhydrostatic compression data [6] since conventional axial x-ray diffraction experiments are performed near this angle. These results show that the inferred compression curve is strongly sensitive to orientation with respect to the loading axis.

Many studies of superhard solids have focused on the more easily measured aggregate elastic properties (e.g., the bulk modulus or, less frequently, the shear modulus) as a proxy for strength [16,17] as the elastic properties are a reflection of bond strength and directionality. However, elastic properties alone are insufficient for complete characterization as shear strength can vary by more than a factor of 10 for materials with comparable shear moduli [16,17]. The hardness may also vary dramatically for materials with similar bulk moduli [16]. A more useful parameter is the ratio of shear strength, τ, to shear modulus, G, which reflects the contributions of both plastic and elastic deformation. Theoretical studies of ideal strengths of solids are typically expressed in terms of τ/G, with values ranging from 0.03–0.04 for fcc metals to values as large as 0.25 for covalently bonded materials [17,28]. In this study, we examine the ratio of t/G, where we expect that at high pressures t has reached its limiting value of 2τ. This ratio can be directly obtained from the average slope of the d spacing vs $1 - 3\cos^2\psi$ relation.

For SiO_2, we find that t/G varies from 0.019(3) to 0.037(5) in the pressure range of 15–60 GPa (Fig. 3).

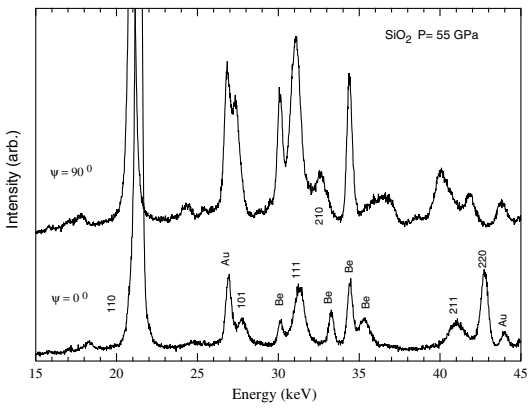

FIG. 1. Energy dispersive x-ray diffraction spectra at maximum strain ($\psi = 0°$) and minimum strain ($\psi = 90°$).

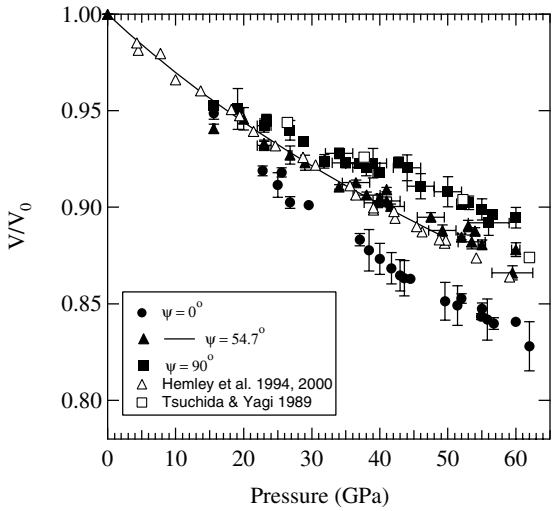

FIG. 2. Equation of state at $\psi = 0°$, 54.7° and 90°. Solid symbols are from this study. Open squares are from Ref. [6] and open triangles are from Refs. [1,14]. The solid line is a fit to our data at $\psi = 54.7°$ using the Birch-Murnaghan equation of state. Error bars are smaller than symbols where not shown .

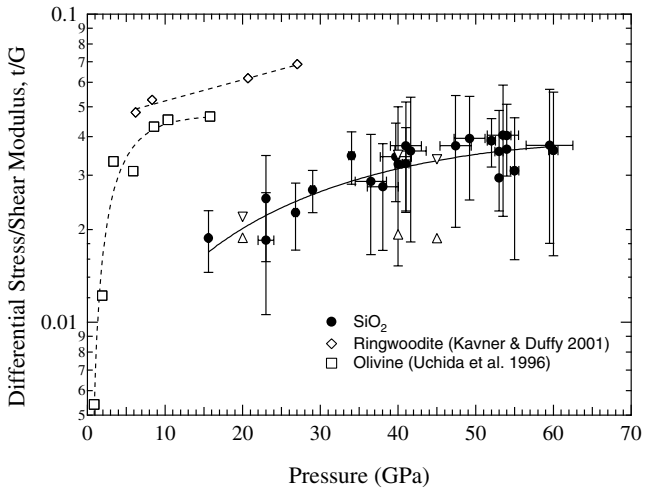

FIG. 3. Ratio of differential stress to shear modulus as a function of pressure. Solid circles denote data from this study. Open squares are from Ref. [29]. Open diamonds are from Ref. [24]. The upward and downward pointing triangles are calculated from the data of Ref. [9] and Ref. [10], respectively (see text for detail).

Despite the increase with pressure, t/G values still lie well below the expected ideal strength for strong brittle solids [28]. There is no observable change in t/G across the expected pressure of the stishovite–$CaCl_2$-type phase transformation ($\sim$50 GPa). Surprisingly, the ratio of differential stress to shear modulus for stishovite is about one-half the value found for olivine (α-Mg_2SiO_4) [29] and ringwoodite (γ-Mg_2SiO_4) [24] at pressures below 30 GPa (Fig. 3). That is, as a fraction of the shear modulus, the differential stress supported by stishovite is significantly less than that of four-coordinated silicates for which t/G values of 0.03–0.07 have been observed [24]. The enhanced hardness of six-coordinate silicates [17], therefore, must primarily reflect the increase in elastic properties across the transition.

In order to quantify the differential stress, it is necessary to estimate the shear modulus. Shear moduli of stishovite have been reported from ultrasonic experiments on polycrystalline aggregates to 10 GPa [19,25] and by theoretical calculations [8,9]. Density functional theory calculations [8,9] show that the elastic moduli C_{11}-C_{12} and, consequently, the Reuss bound shear modulus of stishovite decreases rapidly above 40 GPa and vanishes at approximately 47 GPa. This is the manifestation of the tetragonal shear instability responsible for the softening of the B_{1g} Raman mode [12] and the transition to the orthorhombic $CaCl_2$-type phase [8]. Similar results for the elastic moduli have also been reported from a Landau analysis [10,14] based on a theoretical study [9].

Figure 4 shows the differential stress obtained using the Reuss bound on the shear modulus from the Landau analysis [10]. The differential stress is found to be nearly constant or weakly increasing at pressures of 15–40 GPa and to drop sharply as the transition pressure is approached. The differential stress then recovers rapidly to values of 5 ± 2 GPa at 52–55 GPa in the $CaCl_2$-type phase. Figure 4 also shows that the differential stresses supported by stishovite are significantly lower than those of ringwoodite. This finding is consistent with measurements on SiO_2 glass [18] which show a large reduction in strength as the coordination in the glass increases from fourfold to sixfold during compression. Our results are insensitive to the choice of theoretical model [8–10] for the shear moduli. Using the pressure dependent elastic moduli of Ref. [11] and the expressions for $G_R^X(hkl)$ in the tetragonal system [22], the predicted values of $Q(hkl)$ (for $t = 2.5$–4.5 GPa and $\alpha = 1$) are shown in Fig. 3 (open triangles). Similar results are obtained using the moduli of Ref. [10]. These results show that our lattice strain observations are fully consistent with the elasticity values reported in the theoretical studies.

Application of the lattice strain equations has also been used to directly recover the full elastic stiffness tensor at high pressures for materials in the cubic and hexagonal systems [21–24]. Stishovite crystallizes in the tetragonal system (class $4/mmm$) and thus has six independent elastic stiffnesses (C_{11}, C_{12}, C_{13}, C_{33}, C_{44}, C_{66}). The combination of lattice strain equations [21] for four independent lattice reflections together with expressions for the compressibility and the pressure dependence of the c/a ratio are, in principle, sufficient for recovery of the full elastic tensor. Our inversions on simulated data sets revealed that the lattice strain equations are largely insensitive to C_{44} and C_{66}; hence, these parameters were fixed to theoretical values [9]. We then inverted for the remaining moduli using the (110) and (211) reflections together with the following expressions:

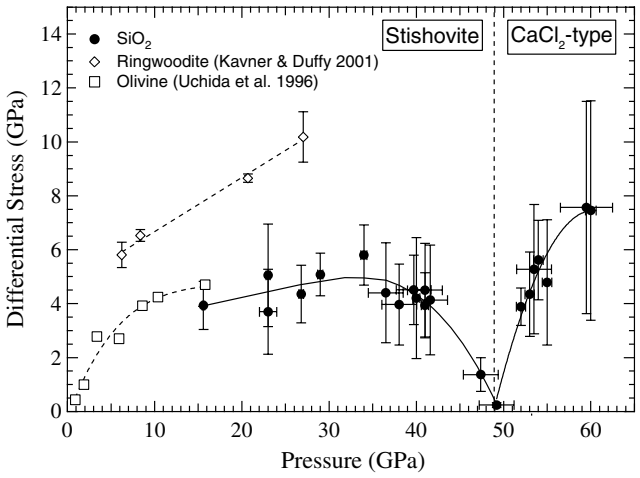

FIG. 4. Differential stress supported by stishovite as a function of pressure. Solid symbols are from this study with a fit to the data shown by the solid line. Open squares and diamonds are from Ref. [29] and Ref. [24], respectively.

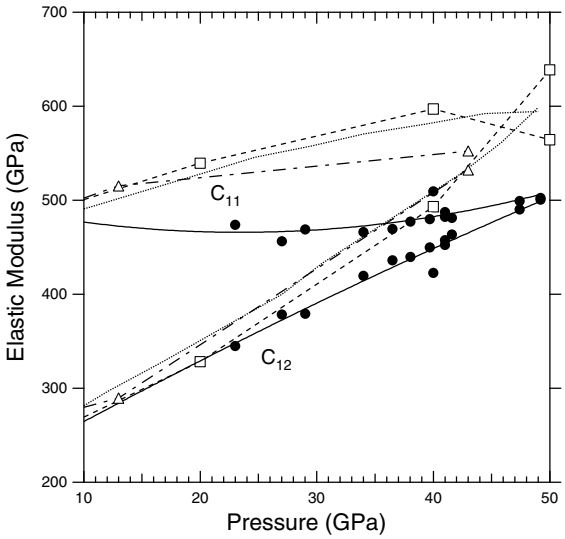

FIG. 5. Elastic moduli as a function of pressure from this study (solid circles and lines) and Refs. [8–10]. Dotted lines, Ref. [10]; open triangles and dash-dotted lines, Ref. [8]; open squares and dashed lines, Ref. [9].

$$1/K = 2S_{11} + 2S_{12} + 4S_{13} + S_{33}, \quad (4)$$

$$d\ln(c/a)/dP = S_{11} + S_{12} - S_{13} - S_{33}, \quad (5)$$

where K is the bulk modulus, a and c are the lattice parameters, and the S_{ij}s are the elastic compliances.

The values for C_{11} and C_{12} are illustrated in Fig. 5, together with theoretical results [8–10]. In general, our values of C_{11} and C_{12} lie below the theoretical studies, but our results are qualitatively consistent with the theoretical studies in that C_{11}-C_{12} is markedly reduced near the phase transition pressure. This result is largely insensitive to the choice of a wide range of t values and shear modulus models. This provides direct experimental support for an elastic instability involving C_{11}-C_{12} in stishovite near 50 GPa.

We thank J. Hu for experimental assistance, S. Speziale, A. Kavner, and A. Singh for helpful discussions, and M. Carpenter for providing his elasticity data. This work was supported by the NSF and the David and Lucile Packard Foundation.

*Electronic address: shieh@princeton.edu

[1] R. J. Hemley, C. T. Prewitt, and K. J. Kingma, *Silica: Physical Behavior, Geochemistry and Material Applications* (Mineralogical Society of America, Washington, D.C., 1994), pp. 41–81.
[2] A. E. Goresy, L. Dubrovinsky, T. G. Sharp, S. K. Saxena, and M. Chen, Science **288**, 1632 (2000).
[3] W. Joswig, T. Stachel, J. Harris, W. Baur, and G. Brey, Earth Planet. Sci. Lett. **173**, 1 (1999).
[4] L. Vinnik, M. Kato, and H. Kawakatsu, Geophys. J. Int. **147**, 41 (2001).
[5] D. Teter, R. J. Hemley, G. Kresse, and J. Hafner, Phys. Rev. Lett. **80**, 2145 (1998).
[6] Y. Tsuchida and T. Yagi, Nature (London) **340**, 217 (1989).
[7] J. Haines, J. Leger, F. Gorelli, and M. Hanfland, Phys. Rev. Lett. **87**, 155503 (2001).
[8] R. E. Cohen, *High Pressure Research: Application to Earth and Planetary Science* (American Geophysical Union, Washington, D.C., 1992), p. 425.
[9] B. B. Karki, L. Stixrude, and J. Crain, Geophys. Res. Lett. **24**, 3269 (1997).
[10] M. A. Carpenter, R. J. Hemley, and H. K. Mao, J. Geophys. Res. **105**, 10 807 (2000).
[11] C. Lee and X. Gonze, Phys. Rev. B **56**, 7321 (1997).
[12] K. J. Kingma, R. E. Cohen, R. J. Hemley, and H. K. Mao, Nature (London) **374**, 243 (1995).
[13] D. Andrault, G. Fiquet, F. Guyot, and M. Hanfland, Science **282**, 720 (1998).
[14] R. J. Hemley, J. Shu, M. A. Carpenter, J. Hu, H. K. Mao, and K. J. Kingma, Solid State Commun. **114**, 527 (2000).
[15] J. M. Leger, J. Haines, M. Schmidt, J. P. Petitet, A. S. Pereira, and J. A. H. da Jornada, Nature (London) **383**, 401 (1996).
[16] V. V. Brazhkin and A. G. Lyapin, JETP Lett. **73**, 197 (2001).
[17] J. Haines, J. Leger, and G. Bocquillon, Annu. Rev. Mater. Sci. **31**, 1 (2001).
[18] C. Meade and R. Jeanloz, Science **241**, 1072 (1988).
[19] B. Li, S. M. Rigden, and R. C. Liebermann, Phys. Earth Planet. Inter. **96**, 113 (1996).
[20] P. Cordier and D. C. Rubie, Mater. Sci. Eng., A **309–310**, 38 (2001).
[21] A. K. Singh, H. K. Mao, R. J. Hemley, and J. Shu, Phys. Rev. Lett. **80**, 2157 (1998).
[22] A. K. Singh, C. Balasingh, H. K. Mao, R. J. Hemley, and J. Shu, J. Appl. Phys. **83**, 7567 (1998).
[23] T. S. Duffy, G. Shen, D. Heinz, J. Shu, Y. Ma, H. Mao, R. J. Hemley, and A. K. Singh, J. Appl. Phys. **60**, 15 063 (1999).
[24] A. Kavner and T. S. Duffy, Geophys. Res. Lett. **28**, 2691 (2001).
[25] B. Li and R. C. Liebermann, Eos Trans. Am. Geophys. Union **82**, 47 (2001).
[26] W. R. Panero, L. R. Benedetti, and R. Jeanloz, J. Geophys. Res. (to be published).
[27] S. N. Luo, J. L. Mosenfelder, P. D. Asimow, and T. J. Ahrens, Geophys. Res. Lett. **29**, 36 (2002).
[28] A. Kelly and N. H. MacMillan, *Strong Solids* (Oxford University Press, New York, 1986), 3rd ed.
[29] T. Uchida, N. Funamori, T. Ohtani, and T. Yagi, *High Pressure Science and Technology* (AIRAPT-15, Poland, 1995), p. 183.